Nanoscale

COMMUNICATION

View Article Online
View Journal | View Issue

Cite this: *Nanoscale*, 2019, **11**, 4712

Received 31st January 2019,
Accepted 25th February 2019

DOI: 10.1039/c9nr01019j

rsc.li/nanoscale

Mechanochemical synthesis of N-doped porous carbon at room temperature†

Mirian Elizabeth Casco, *[a] Sebastian Kirchhoff,[a] Desirée Leistenschneider,[a] Marcus Rauche,[b] Eike Brunner [b] and Lars Borchardt *[a]

We report the one-pot mechanochemical synthesis of N-doped porous carbons at room temperature using a planetary ball mill. The fast reaction (5 minutes) between calcium carbide and cyanuric chloride proceeds in absence of any solvent and displays a facile bottom-up strategy that completely avoids typical thermal carbonization steps and directly yields a N-doped porous carbon containing 16 wt% of nitrogen and exhibiting a surface area of 1080 $m^2 g^{-1}$.

Introduction

Tailoring the microstructure and the electrical properties of carbon-based nanomaterials by molecular design is crucial for many advancing applications[1,2] in fields such as sensors,[3] batteries,[4,5] supercapacitors,[6] electrocatalysis[7,8] or optoelectronics.[9] Doping the π-system of an sp^2-hybridized carbon framework with nitrogen is a straight-forward strategy to increase wettability[10,11] and to enhance catalytic activity (for instance in ORR).[12–14] The comparable size of C and N atoms makes their substitution feasible while the stronger electronegativity of the N changes the electronic properties of the carbon network. Pyridinic nitrogen, for instance, induces Lewis basicity at the adjacent carbon atoms[13] whereas graphitic nitrogen increases the electron density within the delocalized π-system,[15] consequently affecting the electrical conductivity of the graphene network.[16,17]

A growing number of works report N-doping on carbon-based materials by either direct synthesis (*e.g.* chemical vapour deposition,[18,19] solvothermal,[20] arc-discharge,[21] segregation,[22] condensation reaction,[2] thermal decomposition,[23–25] porous polymer precursor approach[26] or post-synthesis approaches (*e.g.* thermal[27,28] or plasma[3] treatment). However, most of these syntheses suffer from a high energy penalty, multiple-step protocols and waste accumulation, which increase production costs considerably. A facile synthesis approach towards N-doped carbon-based materials at industrial quantity, while preserving the environment, is fundamental to guarantee the future commercial application of emerging technologies.

In this context, mechanochemical syntheses have attracted much attention as sustainable and cost-effective alternatives to conventional syntheses for a vast number of products ranging from discrete molecules in organic[29,30] and inorganic[31] chemistry to polymers[32,33] and porous materials.[34,35] These syntheses rely on mechanical energy, which is provided by the collision of milling balls in ball mills, and which is transferred to the chemical educts. These reactions are fast, scalable and can be conducted in a solvent-free environment, reducing waste accumulation to a minimum.

Porous carbons have already been synthesized by mechanochemistry, among them ordered mesoporous carbons,[25,36] and nitrogen-doped carbons.[4,37,38] However, a crucial step in all of these syntheses is a subsequent heat temperature treatment to facilitate carbonization and to derive a graphitic conductive structure. The heat treatment renders not only an additional step but also one of the most energetic steps in the synthesis, probably limiting its applicability.

In order to tackle this drawback, self-sustaining, high-temperature synthesis (SHS) has been investigated to instantaneously form carbon materials from highly exothermic solid state reactions by local heating of the mixture (with a hot wire, electric spark, laser, thermal radiation pulse or ion beam).[39,40] When the reaction is induced by ball milling rather than a preheated solid state mixture, the process is called mechanically-induced self-sustaining reaction (MSR) and is typically performed at room temperature.[41–46] Takacs[47] has nicely reviewed MSR for several systems. Basically, the process consists on a primary activation period during which size reduction; mixing

[a]*Department of Inorganic Chemistry, Technische Universität Dresden, Bergstrasse 66, 01069 Dresden, Germany. E-mail: lars.borchardt@tu-dresden.de, miriancasco@gmail.com*
[b]*Department of Bioanalytical Chemistry, Technische Universität Dresden, Bergstrasse 66, 01069 Dresden, Germany*

†Electronic supplementary information (ESI) available. See DOI: 10.1039/c9nr01019j

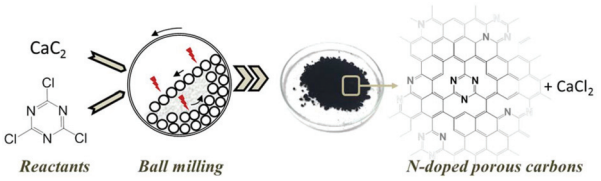

Fig. 1 Concept scheme for the mechanochemical reaction between calcium carbide and cyanuric chloride inside a planetary ball mill at room temperature, resulting in N-doped porous carbons.

and inclusion of defect take place. After this time the mixture ignites and the reaction propagates to form the product in a matter of seconds.

Here we report on the synthesis of a nitrogen-doped carbon *via* MSR at room temperature. We thereby adapt and develop further a recent synthesis concept of our group, the mechanochemical reaction of CaC_2 with halogenated hydrocarbons.[43] In particular, we use the reaction between CaC_2 with cyanuric chloride ($C_3Cl_3N_3$) (Fig. 1). We show that changing the mass ratio of reactants and the milling time allows us to tailor the textural properties and the nitrogen content of the carbonaceous product, reaching values of surface area as high as 1080 $m^2\ g^{-1}$ accompanied with a nitrogen content of 16 wt%.

Materials and methods

Sample preparation

Granular calcium carbide ($CaC_2 \leq 75\%$) was purchased from Sigma Aldrich and ground for 2 h at 500 rpm in a planetary mono mill Pulverisette 6 classic line from Fritsch GmbH. The main impurities of CaC_2 are CaO and $Ca(OH)_2$, although traces of S can also be detected (ESI Fig. 1 and 2†). 99% pure cyanuric chloride ($C_3Cl_3N_3$) was purchased from Sigma Aldrich. The synthesis of the carbonaceous materials was performed by mixing both reactants in a 45 mL zirconium oxide grinding bowl with 22 zirconium oxide balls (d = 10 mm, ~75.7 g) using a planetary micro mill Pulverisette 7 premium line from Fritsch GmbH at the rotational speed of 500 rpm. The system was prepared under argon atmosphere inside a glove box. We tested four different $CaC_2/C_3Cl_3N_3$ mass ratios, namely 0.5, 0.7, 2.3, 4.6. The evolution of pressure and temperature inside the grinding bowl for all samples was monitored by gas pressure and temperature measurement (GTM) automatic system (45 mL zirconium oxide bowl and 22 zirconium oxide balls), see ESI Fig. 3.† After the ignition was detected with the GTM system, the product was milled for 5 min or 120 min, giving 8 samples in total (see ESI Table 1†). The product was washed first with a HCl solution of 10% v/v and then with hot water overnight using soxhlet system until pH = 7 was reached and impurities were removed.

Sample characterization

The nitrogen physisorption isotherms were measured at 77 K using a Quadrasorb EVO/SI apparatus from Quantachrome Instruments. Prior to all measurements, the samples were degassed under vacuum at 150 °C for 12 h. The specific surface area (SSA_{BET}) of the N-doped carbons was calculated using the equation from Brunauer–Emmett–Teller (BET) in the range that fits to the consistency criteria proposed by Rouquerol and Llewellyn.[48] The total pore volume (V_t) was calculated at a relative pressure of 0.95. The sample composition was measured in the CHNS analyser (Euro EA HEKAtech GmbH). Ash content was determined by thermogravimetric analysis (TGA) on a NETZSCH STA 409 C/CD system using alumina crucibles under air stream with the heating rate of 5 °C min^{-1}. Transmission electron microscopy (TEM) image was observed in a JEOL JEM 1400plus operated at an acceleration voltage of 120 kV. The sample were collected by soaking the TEM copper grid in the already with ethanol well-dispersed carbon suspension. Raman spectra were obtained using a Raman-spectrometer DXR SmartRaman from the company Thermo Scientific. The wavelength for the measurement was 532 nm (100 scans). X-ray photoelectron spectroscopy (XPS, K-alpha, Thermo Scientific) was used to analyse the C, N and O species. All spectra were collected using Al-K radiation (1486.6 eV), monochromatized by a twin crystal monochromator, yielding a focused X-ray spot (elliptical in shape with a major axis length of 400 μm) at 3 mA × 12 kV. The alpha hemispherical analyser was operated in the constant energy mode with survey scan pass energies of 200 eV to measure the whole energy band and 50 eV in a narrow scan to selectively measure the particular elements. XPS data were analysed with Avantage software. Electric powder conductivities were measured with an Agilent 34420A combined with a self-constructed cell with a diameter of 1 cm. The powder was pressed with a mass of 2 t.

Results and discussion

Mechanochemical synthesis

In a typical synthesis, the powders of calcium carbide (CaC_2) and cyanuric chloride ($C_3Cl_3N_3$) are placed into a 45 mL zirconia grinding bowl with 22 zirconia milling balls (d = 10 mm, ~75.7 g). After milling at 500 rpm for a certain time and a consecutive washing step, the final N-doped carbon product is obtained. They were labelled as 'N-Carb' following by the $CaC_2/C_3Cl_3N_3$ mass ratio (0.5, 0.7, 2.3 and 4.6). To track the proceeding reaction, we used a vessel with integrated temperature- and pressure-sensors. The evolution of temperature and pressure was recorded for all conditions (Fig. 2) and is characteristic for mechanically-induced self-propagating or self-sustaining reactions.[43–47] At the beginning of the experiment, the pressure remains at atmospheric value and the temperature increases gradually only due to the balls friction. During this time (mechanical induction period), the number of structural defects and the particle surface increase. As a result, the reactivity of the system rises significantly. After the induction time, a sudden rise in the pressure and temperature are detected, which is associated with the instantaneous formation of

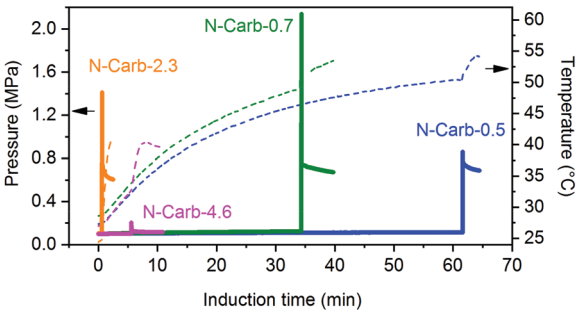

Fig. 2 Temperature (dashed line) and pressure (solid line) profiles for the mechanochemical synthesis of N-doped carbons. Reactions were followed using an easy GTM system (Fritsch GmbH, detailed description ESI Fig. 3†).

carbon. Macroscopically, a black powder is obtained opening the bowl immediately after ignition.

The reactants quantities are selected according to the following hypothetical eqn (1) (symbol for mechanochemical reactivity is adapted from ref. 49). Please, note that this is not a defined stoichiometry. The experimentally obtained composition can be derived from elemental analysis, which will be discussed later.

$$3CaC_2 + 2C_3Cl_3N_3 \xrightarrow{\text{))))}} 3CaCl_2 + 2C_6N_3 \quad (1)$$

A $CaC_2/C_3Cl_3N_3$ mass ratio of 0.7 is calculated to be the stoichiometric quantity, whereas 0.5 corresponds to an excess of $C_3Cl_3N_3$ and 2.3 to an excess of CaC_2 (the purity of CaC_2 75% was taking into account for the calculation). Additionally, we investigated the minimum amount of cyanuric chloride needed to promote the reaction within 1 h, which resulted in a mass ratio of 4.6. Therefore, we can draw two conclusions from comparing the profiles in Fig. 2. Firstly, an excess of CaC_2 promotes the mechanochemical reaction, leading to shorter induction times. This is 1 and 5 min for N-Carb-2.3 and N-Carb-4.6, in contrast to 30 and 60 min for sample N-Carb-0.7 and N-Carb-0.5, respectively. In any of these cases, the necessary times are extremely short compared to conventional carbonization methods to prepare activated carbon materials, which usually require around 2 h plus a cooling period. Note that the registered global temperature rises gradually due to the milling process itself (attrition of milling material) and suddenly shows a small spike (not higher than 50 °C) due to the exothermic nature of the reaction (~−600 kcal). These results demonstrate that, even though the reaction is highly exothermic and provokes a local overheating, the product can be synthesized at room temperature and in a time scale of minutes. The second conclusion is related to the maximal pressure reached by the system during the ignition. The readers have to be aware that this type of reaction can result in an uncontrolled explosion when large quantities of reactants are used in stoichiometric ratios. The pressure rises abruptly due to the expansion wave followed by the propagation reaction front. The remaining pressure might due to the gases formation during the ignition (*e.g.* light hydrocarbons, CO, CO_2), although the currently system does not allow their extraction for further analysis. Oxygen and hydrogen might come from the impurities of calcium carbide (see ESI, S1† for detailed information). In our experiments, the sample N-Carb-0.7 generated a maximal pressure of 2.3 MPa. However, when using an excess of either calcium carbide or cyanuric chloride, the reaction can be controlled and carried out very safely. We observed maximal pressures of 0.1 MPa, 1.4 MPa and 0.9 MPa for samples N-Carb-4.6, N-Carb-2.3 and N-Carb-0.5, respectively. All samples were milled for 5 and 120 min after the detection of the reaction (the milling time was added to the sample's name in subscript, see Table 1). Longer milling time exerts rather low influence on the yield of the reaction (Table 1), which indicates that most of the product is formed during the ignition. In general, the yield

Table 1 Textural and chemical properties of the N-doped porous carbons. The theoretical weight composition of the polymer $(C_6N_3)_n$ (eqn (1)) is 63 wt% C and 37 wt% (C/N = 1.7), while the atomic ratio C/N is 2

						Elemental analysis[f]					XPS[g]			
Materials	Yield[a] (%)	SSA_{BET}[b] ($m^2\ g^{-1}$)	V_{Total}[c] ($cm^3\ g^{-1}$)	Ash[d] (wt%)	I_D/I_G[e] (nm)	N (wt%)	C	H	S	C/N	N (at%)	C	O	C/N
N-Carb-$0.5_{5\ min}$	31	410	0.55	7.2	0.94	12.0	74.7	0.2	0.3	6.2	—	—	—	—
N-Carb-$0.5_{120\ min}$	41	370	0.30	4.8	0.93	18.0	66.7	0.5	0.8	3.7	18.8	74.8	6.1	4.0
N-Carb-$0.7_{5\ min}$	41	170	0.32	7.8	0.66	4.9	83.6	0.1	—	17	—	—	—	—
N-Carb-$0.7_{120\ min}$	43	280	0.20	3.8	1.01	7.0	80.3	—	—	11.5	7.1	88.9	3.8	12.5
N-Carb-$2.3_{5\ min}$	110	230	0.60	6.7	0.92	1.7	81.9	—	—	48.2	—	—	—	—
N-Carb-$2.3_{120\ min}$	98	450	0.36	3.7	1.47	2.0	85.2	0.1	0.8	42.6	1.6	95.2	3.0	53.3
N-Carb-$4.6_{5\ min}$	92	1080	1.00	9.5	0.75	2.2	82.7	0.2	0.7	37.6	—	—	—	—
N-Carb-$4.6_{120\ min}$	110	1080	1.25	2.7	1.13	16.1	60.3	2.1	2.1	3.7	—	—	—	—

[a] Yield (%) = $(m_{final} \times X \times MW_{limiting\ reactant} \times 100)/(m_{limiting\ reactant} \times 2 \times MW_{C_6N_3})$, where X is 3 (or 2) when CaC_2 (or $C_3Cl_3N_3$) is the limiting reactant. MW_{CaC_2} = 64.099 g mol^{-1}. $MW_{C_3Cl_3N_3}$ = 184.41 g mol^{-1}. $MW_{C_6N_3}$ = 114 g mol^{-1}. The yield is calculated according to the hypothetical eqn (1), therefore yields higher than 100% indicates that more acetylene units than expected are reacting. [b] Multi-point BET-method for $0.05 \leq P/P_0 \leq 0.3$. [c] Total pore volume at P/P_0 = 0.95 (N_2 adsorption). [d] Ash content is the remaining mass of thermogravimetric analysis under air. [e] I_D/I_G is the intensities ratio of the D and G peaks. [f] The remaining elemental composition (wt%) is supposed to be oxygen and Ca. [g] The remaining composition (at%) is sulfur coming from the CaC_2.

increases when increasing the calcium carbide content in the initial mixture. However, according to elemental analysis (Table 1), this increment is accompanied with a decrease of the nitrogen content. These opposing observations suggest that CaC_2 can also react with itself to form carbon. Cyanuric chloride, however, is necessary, since milling of pure CaC_2 does not yield any product at all. A proposed mechanism involves the nucleophilic substitution of the anion chloride by the acetylide anion on the triazine ring with the corresponding formation of $CaCl_2$ as a side product. Since triple bond was not found by further structural characterization techniques on the carbon products, the presence of the suggested polymer in eqn (1) can be ruled out. The obtained product is a more stable nitrogen-doped carbon, which structural and textural characteristics will be analyzed along the manuscript. Thermogravimetric analysis shows that the product is stable up to 400 °C in air, with a maximal decomposition rate at around 500–600 °C (see ESI Fig. 4†). The ash content (mainly CaO coming from the calcium carbide impurities) decreases with the milling time (Table 1), since the continuous particle size reduction of the formed carbon allows for a more effective washing process. Traces of S can also be detected in the final carbon by elemental analysis (Table 1).

N-Doped porous carbon

Elemental analysis confirms that nitrogen atoms are incorporated into the carbon network (Table 1). According to the eqn (1), the reaction between calcium carbide and cyanuric chloride might yield a triazine polymer bridged by acetylene units with a theoretical C/N atomic ratio of 2, and a C/N mass ratio of 1.7. However, the experimental results reveal C/N mass ratios between 3.7 and 48, which confirm that the acetylene units react with themselves and the cyanuric chloride is fundamental to start the reaction giving N-doped carbons and $CaCl_2$ as products. A closer look at these values suggests that the nitrogen incorporation process could be divided into two steps: (1) *in situ* doping during the reaction and, (2) *ex situ* doping during the subsequent grinding. The *in situ* doping majorly determines the degree of nitrogen incorporation, which, in principle, is more effective when increasing the amount of cyanuric chloride in the initial mixture. For instance, the nitrogen content is 1.7 wt%, 4.9 wt% and 12 wt% for samples N-Carb-$2.3_{5\ min}$, N-Carb-$0.7_{5\ min}$ and N-Carb-$0.5_{5\ min}$, respectively. The *ex situ* doping, although less effective, still provides further heteroatoms into the carbon network, *e.g.* the nitrogen content for sample N-Carb-$0.5_{5\ min}$ is enhanced from 12 wt% up to 18 wt% after 120 min of milling. In the particular case of N-Carb-4.6, *in situ* doping led to a nitrogen content of 2.2 wt%, that is enhanced up to the value of 16 wt% with the subsequent 120 min of grinding. Please note, that we performed these syntheses several times in order to test the reproducibility of this mechanochemical reaction. As a result, we replicated the product and the nitrogen content, thus confirming the success of the *ex situ* doping for sample N-Carb-4.6.

Structural information about the nitrogen species in the product are obtained by means of X-ray photoelectron spectroscopy (XPS). The survey spectra for samples N-Carb-$0.5_{120\ min}$, N-Carb-$0.7_{120\ min}$ and N-Carb-$2.3_{120\ min}$ are selected and analyzed (Fig. 3a–d). The intensities of the N 1s spectra decrease with the nitrogen content and the C/N ratios are in close agreement with elemental analysis results (Table 1). The fitting of the N 1s spectrum of N-Carb-$0.5_{120\ min}$ reveals three major bands that correspond to pyridinic N (398.8 eV), pyrrolic N (400 eV) and graphitic N (401.1 eV).[50] In the cases of N-Carb-$0.7_{120\ min}$ and N-Carb-$2.3_{120\ min}$ the pyridinic and pyrrolic functionalities dominate in the fitting (Fig. 3c and d). The fitting of the C 1s spectra (see ESI Fig. 5a–c†) reveals two main bands attributed to sp^2 graphitic structure at around 284.6 eV and sp^3 carbon bond at around 285.5 eV; and two minor bands at around 286 eV and 288.5 eV which can be assigned to the C=N double bond and the C–N single bond of the triazine unit, respectively.[51,52] Therefore, the XPS results indicate that triazine units are incorporated into the carbon network, and the doping mainly led to pyridinic species (for more detail about N, C and O species percentages refer to ESI

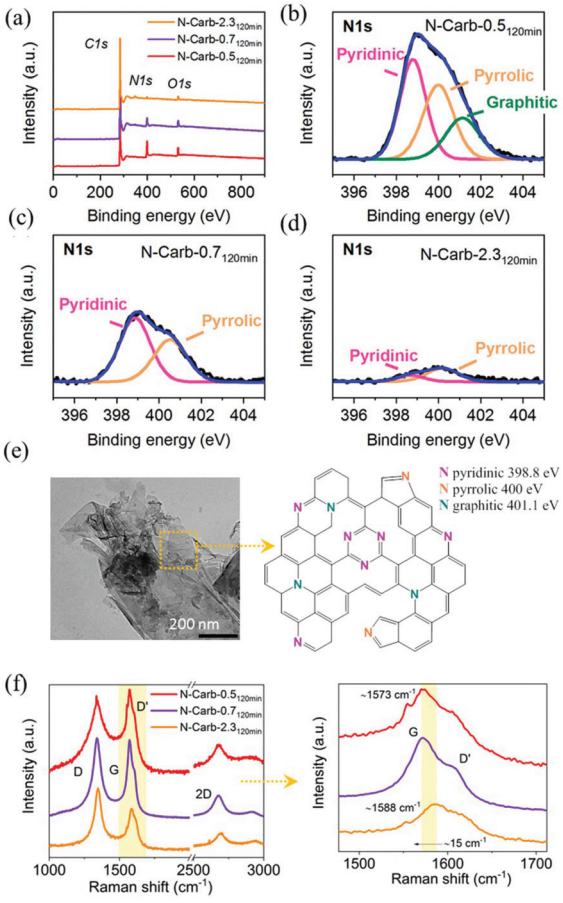

Fig. 3 (a) Survey X-ray photoelectron spectra for samples N-Carb-$X_{120\ min}$ (X = 0.5, 0.7 and 2.3) obtained in the ball mill. N 1s deconvoluted spectra of (b) N-Carb-$0.5_{120\ min}$, (c) N-Carb-$0.7_{120\ min}$ and (d) N-Carb-$2.3_{120\ min}$. (e) Transmission electron microscopy image for sample N-Carb-0.5 and a proposed scheme of a nitrogen-doped graphene layer. (f) Raman spectra for samples N-Carb-$X_{120\ min}$ (X = 0.5, 0.7 and 2.3) obtained in the ball mill and a zoom-in on the G band.

Table 2†). TEM image in Fig. 3e shows a flakes-like microstructure for nitrogen-doped carbon obtained in the ball mill, and a proposed scheme for the N-doped graphene layer with integrated triazine units.

Raman spectra were measured to complement the characterization of the carbon structure (Fig. 3f and ESI Fig. 6†). There was no indication of sp hybridized carbon in the Raman spectra and in turn the existence of the polymer proposed in eqn (1). Three peaks characteristic of carbonaceous materials arise at around 1570–1585 cm^{-1} (G band), 1348 cm^{-1} (D band), and 2688 cm^{-1} (2D). The G band corresponds to the optical mode vibration of two neighbouring carbon atoms on a graphene layer. The D band corresponds to the breathing mode of sp^2 hybridized carbon in the presence of a defect in the aromatic system. In addition, this defect is also responsible for the small shoulder observed on the G peaks at ~1610 cm^{-1} (D′ band).[53] The 2D band, which involves a two-phonon process, is a signature for layer thickness and is related to the number of graphene layers.[54] This peak is sharper for the carbonaceous materials obtained immediately after the ignition (5 min milling time) and becomes smaller after longer milling times due to the inclusions of defects. In addition, a higher I_D/I_G intensities ratio is found when comparing same reactant ratio but higher milling time in parallel with a higher degree of disordering in the sp^2 hybridized carbon network. For N-doped carbon materials, the substitution of C by N atoms must be accompanied by the introduction of defects into the graphene layer.[55] Previous studies from Ferrari and Robertson[55] revealed a down-shift of the G peak position with the nitrogen content. Herein, a maximum shift of ~15 cm^{-1} is observed in the G band position when comparing N-Carb-$0.5_{120\ min}$ (18 wt%N), and N-Carb-$2.3_{120\ min}$ (2 wt%N). This observation supports the XPS results that nitrogen is successfully incorporated into the graphene structure.

The textural properties of the N-doped carbons obtained in the ball mill were investigated by means of nitrogen physisorption technique (see ESI Fig. 7† for N_2 adsorption isotherms and ESI Fig. 8† for pore size distribution). The surface area is between 170 and 1080 $m^2\ g^{-1}$ depending on the mass ratio (Table 1). These surface areas are relatively high considering that neither thermal carbonization nor activation processes were applied. From this, we conclude that mainly the CaC_2 and the graphitization of the acetylene units are responsible for the porosity, while the cyanuric chloride, apart from being C and N source, it is necessary to start the reaction. In addition, we observed that further milling does not affect the textural properties of the materials, but increase considerably the nitrogen content, especially for sample N-Carb-4.6. In consequence, all these results strongly point towards a nitrogen-doped carbon rather than a polymer framework. Moreover, X-ray diffraction reveals the typical pattern for turbostratic carbon (Fig. 4).[56]

We measure the electrical conductivity of the eight samples obtained in the ball mill (Fig. 5). Results reveal a decrease in the conductivity with the milling time. Two factors may explain this trend: the nitrogen content and the surface area. Increasing milling time enhances, at different extent, both of them (Table 1). The high nitrogen content of 16 wt% combined with a surface area of 1080 $m^2\ g^{-1}$ give the lowest electrical conductivity for sample N-Carb-$4.6_{120\ min}$ (0.5×10^{-4} S cm^{-1}). The increasing trend in conductivity of samples N-Carb-0.5, N-Carb-0.7 and N-Carb-2.3, either comparing 5 or 120 min, is in line with the decrease in the nitrogen content. It was reported in the literature the effect of the nitrogen content on the electrical conductivity is determined by a competition between electron doping and structure disorder.[16,57] XPS results demonstrated that mainly pyridinic and pyrrolic species are present in the carbon network, which induce a more defective structure (confirmed by Raman). Nonetheless, the obtained values (Fig. 5) are comparable with that of commercial activated carbons, carbon fibers and carbonized anthracites reported on literature, usually <20 S cm^{-1}.[58] These electrical conductivities are quite good considering that mechanical forces are the only external source of energy.

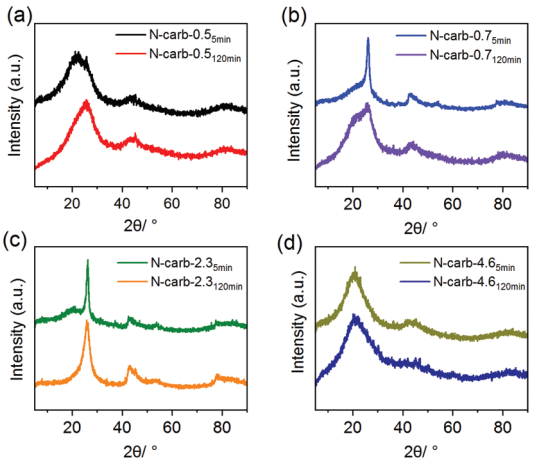

Fig. 4 X-ray diffractograms for the eight N-doped porous carbon materials produced in the ball mill.

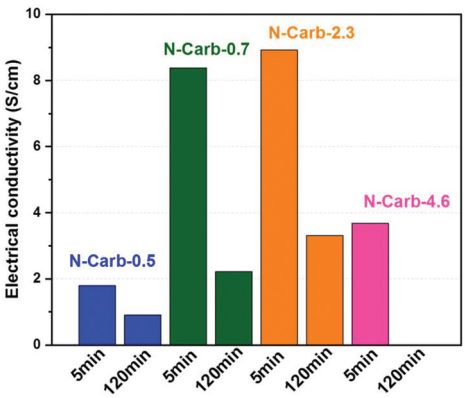

Fig. 5 Electrical conductivities for the eight samples obtained in the ball mill.

Conclusions

We demonstrated that N-doped porous carbons can be synthesized *via* the simple reaction between calcium carbide and cyanuric chloride at room temperature inside a ball mill. We reported further insight into the mechanochemical mechanism. On one side, we found that the cyanuric chloride is critical to start the reaction while *in situ* incorporates nitrogen species, mainly pyridinic. On the other side, we found that the reaction evolves generating the acetylene units to react to each other, and consequently more carbon is produced. Furthermore, the influence of the nitrogen content on the electrical conductivity was investigated. Results show an increment on the electrical conductivity when decreasing the nitrogen content and the surface area. The reported electrical conductivities are quite good considering that any thermal step was avoided; being the mechanical forces the only external source of energy.

Conflicts of interest

There are no conflicts to declare.

Acknowledgements

MEC thanks the Alexander von Humboldt Foundation for financial support. We thank the German Federal Ministry of Education and Research (BMBF) for funding of the "mechanocarb" project (FKZ 03SF0498). Thanks are further due to the Deutsche Forschungsgemeinschaft (grant no. Br 1278/29-1). We thank Christian Kensy (Fraunhofer-IWS) for electrical conductivity measurements, and Prof. Iniesta (University of Alicante) for XPS measurements.

Notes and references

1 H. Wang, T. Maiyalagan and X. Wang, *ACS Catal.*, 2012, **2**, 781.
2 L. Borchardt, Q.-L. Zhu, M. E. Casco, R. Berger, X. Zhuang, S. Kaskel, X. Feng and Q. Xu, *Mater. Today*, 2017, **20**(10), 592.
3 Y. Wang, Y. Shao, D. W. Matson, J. Li and Y. Lin, *ACS Nano*, 2010, **4**, 1790–1798.
4 C. Schneidermann, C. Kensy, P. Otto, S. Oswald, L. Giebeler, D. Leistenschneider, S. Grätz, S. Doerfler, S. Kaskel and L. Borchardt, *ChemSusChem*, 2019, **12**, 310.
5 Y. Xu, C. Zhang, M. Zhou, Q. Fu, C. Zhao, M. Wu and Y. Lei, *Nat. Commun.*, 2018, **9**, 1720.
6 X. Chen, J. Zhang, B. Zhang, S. Dong, X. Guo, X. Mu and B. Fei, *Sci. Rep.*, 2017, **7**, 7362.
7 M. K. Rybarczyk, E. Gontarek, M. Lieder and M.-M. Titirici, *Appl. Surf. Sci.*, 2018, **435**, 543.
8 T. N. Huan, N. Ranjbar, G. Rousse, M. Sougrati, A. Zitolo, V. Mougel, F. Jaouen and M. Fontecave, *ACS Catal.*, 2017, **7**, 1520.
9 T. J. Bandosz and C. O. Ania, *Adv. Sci.*, 2018, **5**, 1800293.
10 W. Tian, H. Li, B. Qin, Y. Xu, Y. Hao, Y. Li, G. Zhang, J. Liu, X. Sun and X. Duan, *J. Mater. Chem. A*, 2017, **5**, 7103.
11 G. P. Hao, G. Mondin, Z. Zheng, T. Biemelt, S. Klosz, R. Schubel, A. Eychmüller and S. Kaskel, *Angew. Chem., Int. Ed.*, 2015, **54**, 1941.
12 Z. Luo, S. Lim, Z. Tian, J. Shang, L. Lai, B. MacDonald, C. Fu, Z. Shen, T. Yu and J. Lin, *J. Mater. Chem.*, 2011, **21**, 8038.
13 D. Guo, R. Shibuya, C. Akiba, S. Saji, T. Kondo and J. Nakamur, *Science*, 2016, **351**, 361.
14 E. Antolini, *Renewable Sustainable Energy Rev.*, 2016, **58**, 34.
15 N. Daems, X. Sheng, I. F. J. Vankelecom and P. P. Pescarmona, *J. Mater. Chem. A*, 2014, **2**, 4085.
16 Z. R. Ismagilov, A. E. Shalagina, O. Y. Podyacheva, A. V. Ischenko, L. S. Kibis, A. I. Boronin, Y. A. Chesalov, D. I. Kochubey, A. I. Romanenko, O. B. Anikeeva, T. I. Buryakov and E. N. Tkachev, *Carbon*, 2009, **47**, 1922.
17 J. R. Pels, F. Kapteijn, J. A. Moulijn, Q. Zhu and K. M. Thomas, *Carbon*, 1995, **33**, 1641.
18 T.-Y. Kim, K.-R. Lee, K. Y. Eun and K.-H. Oh, *Chem. Phys. Lett.*, 2003, **372**, 603.
19 X. Yongde and R. Mokaya, *Chem. Mater.*, 2005, **17**(6), 1553.
20 D. Deng, X. Pan, L. Yu, Y. Cui, Y. Jiang, J. Qi, W.-X. Li, Q. Fu, X. Ma, Q. Xue, G. Sun and X. Bao, *Chem. Mater.*, 2011, **23**, 1188.
21 N. Li, Z. Wang, K. Zhao, Z. Shi, Z. Gu and S. Xu, *Carbon*, 2010, **48**, 255.
22 C. Zhang, L. Fu, N. Liu, M. Liu, Y. Wang and Z. Liu, *Adv. Mater.*, 2011, **23**, 1020.
23 R. J. White, M. Antonietti and M.-M. Titirici, *J. Mater. Chem.*, 2009, **19**, 8645.
24 S. J. Yang, R. Rothe, S. Kirchhecker, D. Esposito, M. Antonietti, H. Gojzewski and N. Fechler, *Carbon*, 2015, **94**, 641.
25 E. Zhang, G.-P. Hao, M. E. Casco, V. Bon, S. Grätz and L. Borchardt, *J. Mater. Chem. A*, 2018, **6**, 859.
26 J. Zhu, C. Yang, C. Lu, F. Zhang, Z. Yuan and X. Zhuang, *Acc. Chem. Res.*, 2018, **51**(12), 3191.
27 L.-S. Zhang, X.-Q. Liang, W.-G. Song and Z.-Y. Wu, *Phys. Chem. Chem. Phys.*, 2010, **12**, 12055.
28 Z.-H. Sheng, L. Shao, J.-J. Chen, W.-J. Bao, F.-B. Wang and X.-H. Xia, *ACS Nano*, 2011, **5**, 4350.
29 J. G. Hernández and C. Bolm, *J. Org. Chem.*, 2017, **82**, 4007.
30 J. L. Howard, Q. Cao and D. L. Browne, *Chem. Sci.*, 2018, **9**, 3080.
31 J. Puszkiel, F. C. Gennari, P. Arneodo Larochette, H. E. Troiani, F. Karimi, C. Pistidda, R. Gosalawit-Utke, J. Jepsen, T. R. Jensen, C. Gundlach, M. Tolkiehn, J. Bellosta Von Colbe, T. Klassen and M. Dornheim, *J. Power Sources*, 2014, **267**, 799.
32 E. Troschke, S. Grätz, T. Lübken and L. Borchardt, *Angew. Chem., Int. Ed.*, 2017, **56**, 6859.

33 S. Grätz and L. Borchardt, *RSC Adv.*, 2016, **6**, 64799.
34 P. A. Julien, K. Užarević, A. D. Katsenis, S. A. J. Kimber, T. Wang, O. K. Farha, Y. Zhang, J. Casaban, L. S. Germann, M. Etter, R. E. Dinnebier, S. L. James, I. Halasz and T. Friščić, *J. Am. Chem. Soc.*, 2016, **138**, 2929.
35 K. Užarević, T. C. Wang, S.-Y. Moon, A. M. Fidelli, J. T. Hupp, O. K. Farha and T. Friščić, *Chem. Commun.*, 2016, **52**, 2133.
36 D. Leistenschneider, N. Jäckel, F. Hippauf, V. Presser and L. Borchardt, *Beilstein J. Org. Chem.*, 2017, **13**, 1332.
37 C. Schneidermann, N. Jäckel, S. Oswald, L. Giebeler, V. Presser and L. Borchardt, *ChemSusChem*, 2017, **10**, 2416.
38 O. S. G. P. Soares, R. P. Rocha, A. G. Gonçalves, J. L. Figueiredo, J. J. M. Órfão and M. F. R. Pereira, *Carbon*, 2015, **91**, 114.
39 S. Dyjak, W. Kiciński, M. Norek, A. Huczko, O. Łabędź, B. Budner and M. Polański, *Carbon*, 2016, **96**, 937.
40 M. Szala, *Fullerenes, Nanotubes, Carbon Nanostruct.*, 2013, **21**(10), 879.
41 G. Cao, S. Doppiu, M. Monagheddu, R. Orru, M. Sannia and G. Cocco, *Ind. Eng. Chem. Res.*, 1999, **38**, 3218.
42 Q. Li, C. Yang, L. Wu, H. Wang and X. Cui, *J. Mater. Chem. A*, 2019, DOI: 10.1039/C8TA10317H.
43 M. E. Casco, F. Badaczewski, S. Grätz, A. Tolosa, V. Presser, B. M. Smarsly and L. Borchardt, *Carbon*, 2018, **139**, 325.
44 A. Popovich, V. P. Reva, V. N. Vasilenko and O. A. Belous, *Mater. Sci. Forum*, 1992, **88–90**, 737.
45 C. Deidda, F. Delogu and G. Cocco, *J. Mater. Sci.*, 2004, **39**, 5315.
46 G. Mulas, S. Loiselle, L. Schiffini and G. Cocco, *J. Solid State Chem.*, 1997, **129**, 263.
47 L. Takacs, *Prog. Mater. Sci.*, 2002, **47**, 355.
48 J. Rouquerol, P. Llewellyn and F. Rouquerol, *Stud. Surf. Sci. Catal.*, 2007, **160**, 49.
49 N. R. Rightmire and T. P. Hanusa, *Dalton Trans.*, 2016, **45**, 2352.
50 P. Hammer and F. Alvarez, *Thin Solid Films*, 2001, **398–399**, 116.
51 U. Gelius, C. J. Allan, G. Johansson, H. Siegbahn, D. A. Allison and K. Siegbahn, *Phys. Scr.*, 1971, **3**, 237.
52 A. Snis, S. F. Matar, O. Plashkevych and H. Ågren, *J. Chem. Phys.*, 1999, **111**, 9678.
53 A. C. Ferrari and D. M. Basko, *Nat. Nanotechnol.*, 2013, (8), 235.
54 L. M. Malard, M. A. Pimenta, G. Dresselhaus and M. S. Dresselhaus, *Phys. Rep.*, 2009, **473**, 51.
55 A. C. Ferrari and J. Robertson, *Philos. Trans. R. Soc., A*, 2004, **362**, 2477.
56 J. Biscoe and B. E. Warren, *J. Appl. Phys.*, 1942, **13**, 364.
57 M. Einert, C. Wessel, F. Badaczewski, T. Leichtweiß, C. Eufinger, J. Janek, J. Yuan, M. Antonietti and B. M. Smarsly, *Macromol. Chem. Phys.*, 2015, **216**, 1930.
58 N. Rey-Raap, E. G. Calvo, J. M. Bermúdez, I. Cameán, A. B. García, J. A. Menéndez and A. Arenillas, *Measurement*, 2014, **56**, 215.